IOP Publishing Measurement Science and Technology
Meas. Sci. Technol. 31 (2020) 055010 (9pp) https://doi.org/10.1088/1361-6501/ab62c6

A new large-scale posture measurement system based on a six-laser tracer multilateral method

Jihui Zheng[1,2], Dongjing Miao[2], Jianshuang Li[2], Shuai Zhang[2] and Baixing Fan[3]

[1] State Key Lab of Precision Measuring Technology and Instruments, Tianjin University, Tianjin 300072, People's Republic of China
[2] Division of Metrology in Length and Precision Engineering, National Institute of Metrology, China, Beijing 100029, People's Republic of China
[3] Institute of Geographical Spatial Information, Information Engineering University, Zhengzhou 450001, People's Republic of China

E-mail: miaodj@nim.ac.cn

Received 23 September 2019, revised 17 November 2019
Accepted for publication 17 December 2019
Published 6 February 2020

Abstract

To realize high-accuracy posture measurement in large scale, a posture measurement system is proposed in this study based on a six-laser multilateral method, mainly composed of six laser tracers and three reflectors—a different number of laser tracers tracks each mirror. But in this state, the system is positive definite, and it cannot achieve the system parameters by self-calibration. To solve this problem, a stepwise calibration method to obtain the system parameters by three-step calibration is presented. Simulations and experiments are carried out to verify the effectiveness of the proposed method. The experimental results show that the posture errors are distributed over [−13.6″, 6.6″] when the measurement range is [5 m, 7 m], which shows that the new measurement system has a high posture measurement accuracy in large scale.

Keywords: metrology, laser multilateral method, stepwise calibration, posture measurement, large scale

(Some figures may appear in colour only in the online journal)

1. Introduction

High-accuracy posture measurement technology in large space is the continuous pursuit of large-scale equipment manufacturing fields such as aviation, aerospace, automobiles, ships, etc [1, 2].

At present, the main methods of posture measurement are machine vision [3, 4], laser radars [5], total stations [6], laser trackers [7–9] and wMPS (workshop measurement and positioning system) [10, 11]. The machine vision measurement system has the advantages of non-contact measurement, and its posture measurement accuracy is about 0.5° in the large-scale field. wMPS is a non-contact measurement with a fast measurement speed, and the accuracy of posture measurement is better than 0.07°, but it is challenging to achieve high posture measurement accuracy with this system.

Huo *et al* [12] proposed a posture measurement method of laser projection imaging. A high-speed camera was used to record the position of a projected light spot in real-time and to establish the posture calculation model of the moving target. The position accuracy was 5 mm, and the attitude angle accuracy was 1′ in a field of 14 m × 7 m. Tian *et al* [13] used a high precision theodolite to measure several feature points on the target, and fitted the target posture by using the least squares method. It was proven that the calibration accuracy could reach 0.05°.

The measuring system based on the principle of the multilateral laser method has the characteristics of a broad space

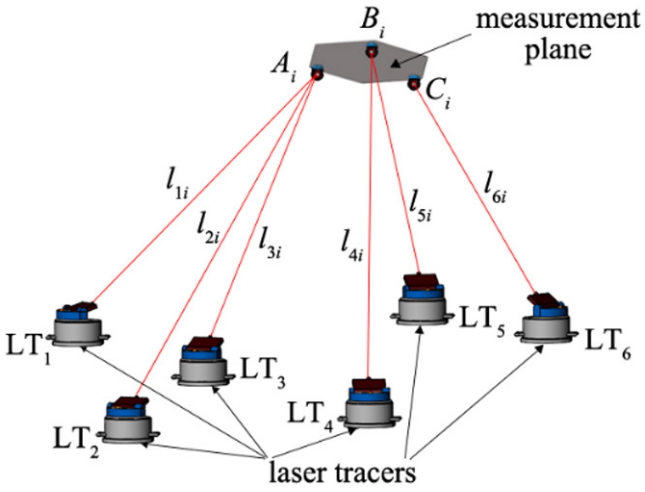

Figure 1. Measuring principle of the six-laser tracer multilateral posture measuring system.

measurement range, high accuracy, substantial flexibility, and firm dynamics, and it has a broad application prospect. Now the laser multilateral measurement system has played an essential role in the field of large-scale coordinate measurement [14–16]. The measurement process only involves the measurement of the length, not the measurement of angle information,and the length accuracy measured by laser interference is high so that the measurement system has high efficiency. Physikalisch-Technische Bundesanstalt [17] used four laser tracking interferometers to form the M3D3 measuring system. In space, an independent laser interferometer is used for a distance test. Tests revealed that the length measurement uncertainty is less than 0.4 μm within a measurement volume of 1 m^3. The National Institute of Metrology, China (NIM) [18] researched the laser multilateral coordinate measurement system. The experiments showed that the coordinate errors are less than 8.9 μm in 1.4 m × 3.7 m × 1.3 m rectangular space. To realize the measurement from three dimensions to six dimensions, the laser triangulation method is extended to a new method for posture measurement.

2. Posture measurement principle: six-laser multilateral measurement system

Before this, NIM used seven laser tracers to realize posture analysis. Simulations show that with an increase of the number of measurement planes, the plane angle error was reduced from 145″ to 3″ [19].

Through modeling and formula derivation, a new method consisting of a six-laser multilateral posture measurement is proposed. This new method eliminates one device and realizes posture measurement. As shown in figure 1, there are six laser tracers LT_1, …, LT_6 in the posture measurement system. The commercial laser tracer is produced by Etalon AG and the measurement uncertainty for the length displacement of the laser tracer is 0.2 μm + 0.3 μm m^{-1}. Three reflectors—*A*, *B*, *C*—are fixed on the measuring target.

LT_1, LT_2 and LT_3 track *A*, LT_4 and LT_5 track *B*, and LT_6 tracks *C*. Distance variations of each laser tracer are taken as

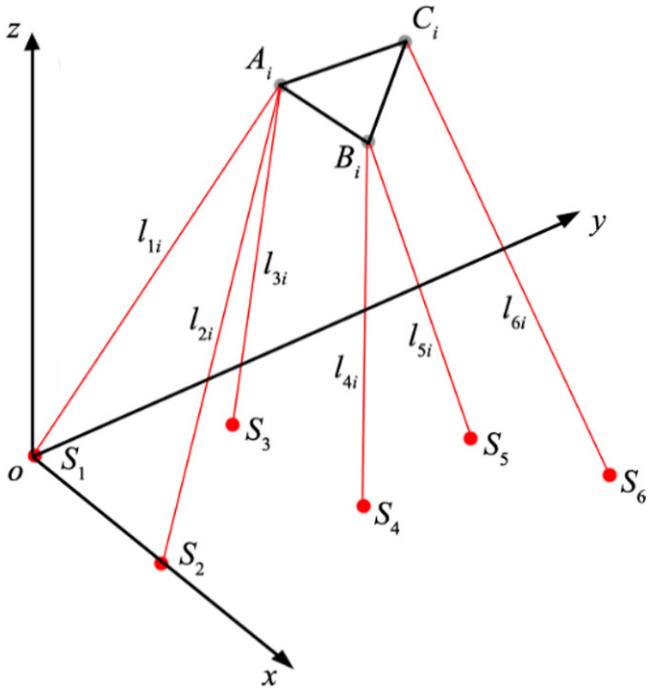

Figure 2. Establishing the special coordinate system.

part of the optimization functions when moving the measurement plane. Then, the system parameters are obtained by the least-squares algorithm. When the posture measurement system is built, it is necessary to calibrate the system parameters to determine the position relation between multiple instruments. However, in this state, the system is positive definite and cannot realize the self-calibration of the system parameters. To solve this problem, we propose a stepwise calibration method whereby system parameters are obtained by three-step calibration—the specific techniques are described in section 3.

3. Stepwise calibration of the system parameters

As shown in figure 2, a special coordinate system is established for six laser tracers. $S_1, \cdots, S_6$ are the measurement centers of the six laser tracers, respectively, where $A_i(x_{A_i}, y_{A_i}, z_{A_i})$, $B_i(x_{B_i}, y_{B_i}, z_{B_i})$, $C_i(x_{C_i}, y_{C_i}, z_{C_i})$ are the optical centers of the reflectors at the measurement position *i*. S_1 is set as the origin of the global coordinate system, S_2 is defined as the *X* axis, S_3 is located at plane *XOY*, so S_1, S_2, S_3, S_4, S_5, S_6 are denoted as $(0,0,0)$, $(x_{S_2},0,0)$, $(x_{S_3},y_{S_3},0)$, $(x_{S_4},y_{S_4},z_{S_4})$, $(x_{S_5},y_{S_5},z_{S_5})$, $(x_{S_6},y_{S_6},z_{S_6})$. l_{1i}, l_{2i}, l_{3i} are the lengths from A_i to S_1, S_2, S_3; l_{4i}, l_{5i} are the lengths from B_i to S_4, S_5; l_{6i} is the length from C_i to S_6. Before measurement, $l_{10}, \ldots, l_{60}$ are unknown parameters to be calibrated. The centers of the laser tracers $S_2, \ldots, S_6$ contain the unknown parameters to be calibrated. There are 18 parameters which need to be calibrated, which include l_{10}, l_{20}, l_{30}, l_{40}, l_{50}, l_{60}, x_{S_2}, x_{S_3}, y_{S_3}, x_{S_4}, y_{S_4}, z_{S_4}, x_{S_5}, y_{S_5}, z_{S_5}, x_{S_6}, y_{S_6}, z_{S_6}.

Since there is no redundant information in the six-laser multilateral posture measuring system, it cannot directly complete self-calibration in the above tracking state. To complete

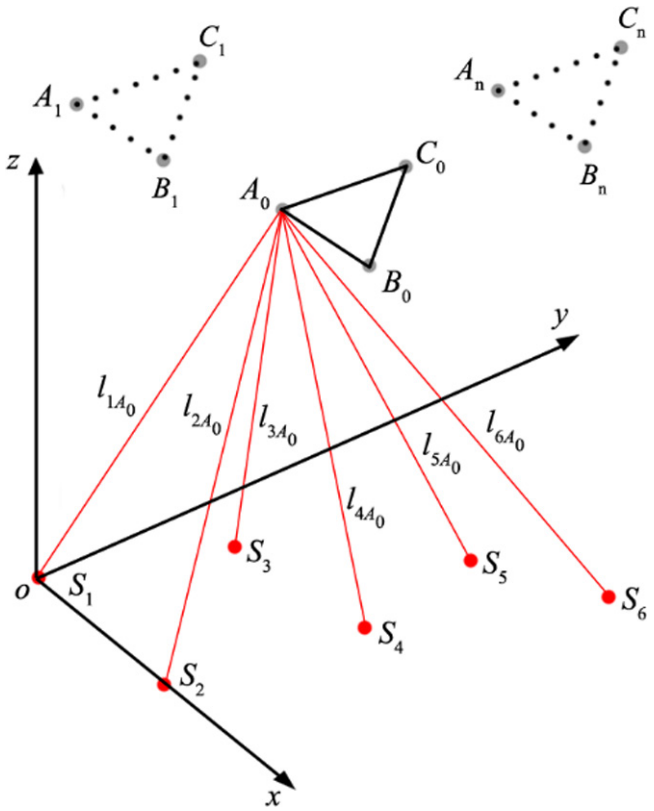

Figure 3. Six laser tracers track reflector A at the same time.

the calibration of the system parameters, we propose a stepwise calibration method. It is necessary to use six laser tracers to track reflector A at the same time, and then track reflector B and C using the following three steps to realize the stepwise calibration of the system parameters:

Firstly, as shown in figure 3, the six laser tracers track reflector A at the same time. The coordinates of the six laser tracer measuring centers $S_{j,A}, j = 1, \ldots, 6$ are denoted as $\left(x_{S_{j,A}}, y_{S_{j,A}}, z_{S_{j,A}}\right), j = 1, \ldots, 6$. The lengths from the reflector center A located at an initial position to the six laser tracers denoted as $l_{jA_0}, j = 1, \ldots, 6$. There are 18 parameters of A which need to be calibrated which include l_{1A_0}, l_{2A_0}, l_{3A_0}, l_{4A_0}, l_{5A_0}, l_{6A_0}, $x_{S_{2,A}}$, $x_{S_{3,A}}$, $y_{S_{3,A}}$, $x_{S_{4,A}}$, $y_{S_{4,A}}$, $z_{S_{4,A}}$, $x_{S_{5,A}}$, $y_{S_{5,A}}$, $z_{S_{5,A}}$, $x_{S_{6,A}}$, $y_{S_{6,A}}$, $z_{S_{6,A}}$ at this time. We set a three-layer measuring plane in space, and the reflector moves on the measuring plane, each flat surface uniformly distributing measuring points. For each position $A_i(x_{A_i}, y_{A_i}, z_{A_i})$ and the measuring centers of the six laser tracers $S_{j,A}(x_{S_{j,A}}, y_{S_{j,A}}, z_{S_{j,A}}), j = 1, \ldots, 6$, the equation $f_{A_i,j}$ is listed as follows [20]:

$$f_{A_i,j} = \left(x_{A_i} - x_{S_{j,A}}\right)^2 + \left(y_{A_i} - y_{S_{j,A}}\right)^2 + \left(z_{A_i} - z_{S_{j,A}}\right)^2 - \left(l_{jA_0} + \Delta l_{jA_i}\right)^2. \tag{2.1}$$

When the number of points in space is sufficient, there are 18 parameters of A which can be calibrated by minimizing $\varnothing_A(x)$ in the following equation [21]:

$$\varnothing_A(x) = \frac{1}{2}\sum_{i=1}^{n} f_{A_i,j}^2(x). \tag{2.2}$$

Secondly, six laser tracers track reflector B at the same time. The coordinates of the six laser tracer measuring centers $S_{j,B}, j = 1, \ldots, 6$ are denoted as $(x_{S_{j,B}}, y_{S_{j,B}}, z_{S_{j,B}})$, and the lengths from the reflector center B_0 are located at an initial position to the six laser tracers denoted as l_{jB_0}. There are 18 parameters of B which need to be calibrated, including l_{1B_0}, l_{2B_0}, l_{3B_0}, l_{4B_0}, l_{5B_0}, l_{6B_0}, $x_{S_{2,B}}$, $x_{S_{3,B}}$, $y_{S_{3,B}}$, $x_{S_{4,B}}$, $y_{S_{4,B}}$, $z_{S_{4,B}}$, $x_{S_{5,B}}$, $y_{S_{5,B}}$, $z_{S_{5,B}}$, $x_{S_{6,B}}$, $y_{S_{6,B}}$, $z_{S_{6,B}}$ at this time. The method of parameter solving is the same as tracking reflector A.

Thirdly, six laser tracers track reflector C at the same time. The coordinates of the six laser tracer measuring centers $S_{j,C}, j = 1, \ldots, 6$ are denoted as $(x_{S_{j,C}}, y_{S_{j,C}}, z_{S_{j,C}})$, and the lengths from the reflector center C_0 are located at an initial position to the six laser tracers denoted as l_{jC_0}. There are 18 parameters of C which need to be calibrated, including l_{1C_0}, l_{2C_0}, l_{3C_0}, l_{4C_0}, l_{5C_0}, l_{6C_0}, $x_{S_{2,C}}$, $x_{S_{3,C}}$, $y_{S_{3,C}}$, $x_{S_{4,C}}$, $y_{S_{4,C}}$, $z_{S_{4,C}}$, $x_{S_{5,C}}$, $y_{S_{5,C}}$, $z_{S_{5,C}}$, $x_{S_{6,C}}$, $y_{S_{6,C}}$, $z_{S_{6,C}}$ at this time. The method of parameter solving is the same as tracking reflector A.

Then, the system parameters are as follows:

$$x_{S_j} = \left(\frac{x_{S_{j,A}} + x_{S_{j,B}} + x_{S_{j,C}}}{3}\right), j = 1, \ldots, 6 \tag{2.3}$$

$$y_{S_j} = \left(\frac{y_{S_{j,A}} + y_{S_{j,B}} + y_{S_{j,C}}}{3}\right), j = 1, \ldots, 6 \tag{2.4}$$

$$z_{S_j} = \left(\frac{z_{S_{j,A}} + z_{S_{j,B}} + z_{S_{j,C}}}{3}\right), j = 1, \ldots, 6 \tag{2.5}$$

$$l_{j0} = l_{jA_0}, j = 1, 2, 3 \tag{2.6}$$

$$l_{j0} = l_{jB_0}, j = 4, 5 \tag{2.7}$$

$$l_{60} = l_{6C_0}. \tag{2.8}$$

After the system parameters are calibrated, LT_1, LT_2 and LT_3 track A, LT_4 and LT_5 track B, and LT_6 tracks C. We calibrate the lengths l_{AB}, l_{AC}, l_{BC} between each reflector in advance. A measuring plane is put on a high precision turntable, and then we rotate the turntable to form different posture measuring planes. When moving the measuring plane, the distance variations of the laser tracers are measured. Among the nine formulas (2.9)–(2.14), only the coordinate value of $A_i(x_{A_i}, y_{A_i}, z_{A_i})$, $B_i(x_{B_i}, y_{B_i}, z_{B_i})$, $C_i(x_{C_i}, y_{C_i}, z_{C_i})$ is unknown, and the other parameters have been calibrated. Therefore, the coordinate of A_i, B_i, C_i on the measurement plane can be calculated by the formula:

$$f_{i,j} = \left(x_{A_i} - x_{S_j}\right)^2 + \left(y_{A_i} - y_{S_j}\right)^2 + \left(z_{A_i} - z_{S_j}\right)^2 - \left(l_{j0} + \Delta l_{ji}\right)^2, j = 1, 2, 3 \tag{2.9}$$

$$f_{i,j} = \left(x_{B_i} - x_{S_j}\right)^2 + \left(y_{B_i} - y_{S_j}\right)^2 + \left(z_{B_i} - z_{S_j}\right)^2 - \left(l_{j0} + \Delta l_{ji}\right)^2, j = 4, 5 \tag{2.10}$$

$$f_{i,6} = \left(x_{C_i} - x_{S_6}\right)^2 + \left(y_{C_i} - y_{S_6}\right)^2 + \left(z_{C_i} - z_{S_6}\right)^2 - \left(l_{60} + \Delta l_{6i}\right)^2 \tag{2.11}$$

$$f_{i,7} = (x_{A_i} - x_{B_i})^2 + (y_{A_i} - y_{B_i})^2 + (z_{A_i} - z_{B_i})^2 - l_{AB}^2 \tag{2.12}$$

$$f_{i,8} = (x_{A_i} - x_{C_i})^2 + (y_{A_i} - y_{C_i})^2 + (z_{A_i} - z_{C_i})^2 - l_{AC}^2 \tag{2.13}$$

$$f_{i,9} = (x_{B_i} - x_{C_i})^2 + (y_{B_i} - y_{C_i})^2 + (z_{B_i} - z_{C_i})^2 - l_{BC}^2. \tag{2.14}$$

The A_i, B_i, C_i coordinates are measured and used to calculate the posture of the measuring plane. Six parameters are needed to determine the posture of the measuring plane: three translation coordinates (expressed by point A_i) and three rotation angles (expressed by pitch angle α_i, yaw angle β_i, and roll angle γ_i).

We create a new coordinate system UVW on the measurement plane. A_i is set as the origin of the new coordinate system UVW, and $\overrightarrow{A_iB_i}$ is defined as the U axis. So, the unit vector $\overrightarrow{u_i}$, $\overrightarrow{v_i}$, $\overrightarrow{w_i}$ can be expressed as

$$\overrightarrow{u_i} = \frac{\overrightarrow{A_iB_i}}{\left|\overrightarrow{A_iB_i}\right|} \tag{2.15}$$

$$\overrightarrow{v_i} = \frac{\overrightarrow{A_iC_i} \times \overrightarrow{A_iB_i}}{\left|\overrightarrow{A_iC_i} \times \overrightarrow{A_iB_i}\right|} \tag{2.16}$$

$$\overrightarrow{w_i} = \overrightarrow{u_i} \times \overrightarrow{v_i}. \tag{2.17}$$

When the XYZ coordinate system is converted to the UVW coordinate system, it needs to undergo rotation and translation changes. The translation transformation matrix $T(x_{A_i}, y_{A_i}, z_{A_i})$ is expressed as

$$T(x_{A_i}, y_{A_i}, z_{A_i}) = \begin{bmatrix} 1 & 0 & 0 & x_{A_i} \\ 0 & 1 & 0 & y_{A_i} \\ 0 & 0 & 1 & z_{A_i} \\ 0 & 0 & 0 & 1 \end{bmatrix}. \tag{2.18}$$

Pitch angle α_i is the angle by which the X axis needs to rotate during the transformation, and its rotation matrix is expressed as

$$\mathrm{Rot}(x, \alpha_i) = \begin{bmatrix} 1 & 0 & 0 & 0 \\ 0 & \cos\alpha_i & -\sin\alpha_i & 0 \\ 0 & \sin\alpha_i & \cos\alpha_i & 0 \\ 0 & 0 & 0 & 1 \end{bmatrix}. \tag{2.19}$$

Yaw angle β_i is the angle by which the Y axis needs to rotate during the transformation, and its rotation matrix is expressed as

$$\mathrm{Rot}(y, \beta_i) = \begin{bmatrix} \cos\beta_i & 0 & \sin\beta_i & 0 \\ 0 & 1 & 0 & 0 \\ -\sin\beta_i & 0 & \cos\beta_i & 0 \\ 0 & 0 & 0 & 1 \end{bmatrix}. \tag{2.20}$$

Roll angle γ_i is the angle by which the Z axis needs to rotate during the transformation, and its rotation matrix is expressed as

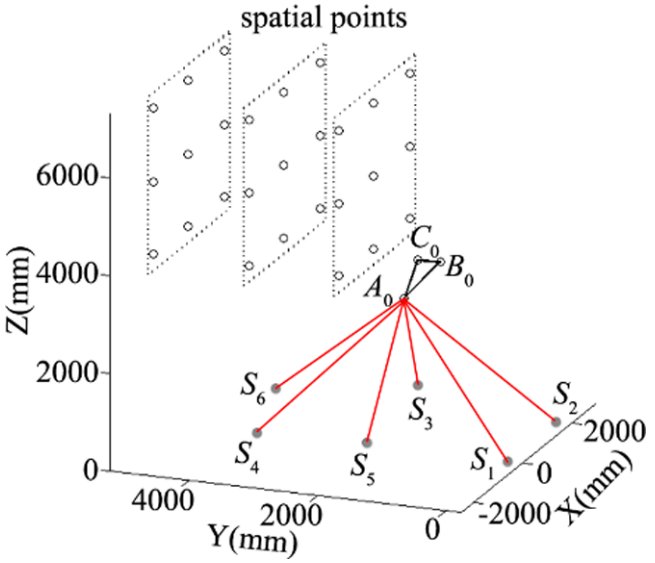

Figure 4. Self-calibration points for simulations.

$$\mathrm{Rot}(z, \gamma_i) = \begin{bmatrix} cos\gamma_i & -\sin\gamma_i & 0 & 0 \\ \sin\gamma_i & \cos\gamma_i & 0 & 0 \\ 0 & 0 & 1 & 0 \\ 0 & 0 & 0 & 1 \end{bmatrix}. \tag{2.21}$$

Then we can obtain the coordinate transformation matrix as

$$\begin{aligned} \mathrm{TR}_i &= T(x_{A_i}, y_{A_i}, z_{A_i})\mathrm{Rot}(z, \gamma_i)\mathrm{Rot}(y, \beta_i)\mathrm{Rot}(x, \alpha_i) \\ &= \begin{bmatrix} \cos\gamma_i\sin\beta_i & \cos\gamma_i\sin\beta_i\sin\alpha_i - \sin\gamma_i\cos\alpha_i \\ \sin\gamma_i\cos\beta_i & \sin\gamma_i\sin\beta_i\sin\alpha_i + \cos\gamma_i\cos\alpha_i \\ -\sin\beta_i & \cos\beta_i\sin\alpha_i \\ 0 & 0 \end{bmatrix} \\ &\quad \begin{bmatrix} \cos\gamma_i\sin\beta_i\cos\alpha_i + \sin\gamma_i\sin\alpha_i & x_{A_i} \\ \sin\gamma_i\sin\beta_i\cos\alpha_i - \cos\gamma_i\sin\alpha_i & y_{A_i} \\ \cos\beta_i\cos\alpha_i & z_{A_i} \\ 0 & 1 \end{bmatrix}. \end{aligned} \tag{2.22}$$

The unit vector $\vec{x}, \vec{y}, \vec{z}$ of the XYZ coordinate system is (1,0,0), (0,1,0) and (0,0,1). Unit vector $(\vec{x}, \vec{y}, \vec{z})$ can obtain $(\overrightarrow{u_i}, \overrightarrow{v_i}, \overrightarrow{w_i})$ after rotation translation transformation:

$$\begin{bmatrix} u_{xi} & v_{xi} & w_{xi} & x_{A_i} \\ u_{yi} & v_{yi} & w_{yi} & y_{A_i} \\ u_{zi} & v_{zi} & w_{zi} & z_{A_i} \\ 0 & 0 & 0 & 1 \end{bmatrix} = \mathrm{TR}_i \begin{bmatrix} 1 & 0 & 0 & 0 \\ 0 & 1 & 0 & 0 \\ 0 & 0 & 1 & 0 \\ 0 & 0 & 0 & 1 \end{bmatrix}. \tag{2.23}$$

Pitch α_i, yaw β_i and roll γ_i can be calculated by formula (2.23)

$$\alpha_i = \arcsin\left(\frac{v_{zi}}{\sqrt{1 - u_{zi}^2}}\right) \tag{2.24}$$

$$\beta_i = \arcsin\left(-u_{zi}\right) \tag{2.25}$$

$$\gamma_i = \arcsin\left(\frac{u_{yi}}{\sqrt{1 - u_{zi}^2}}\right). \tag{2.26}$$

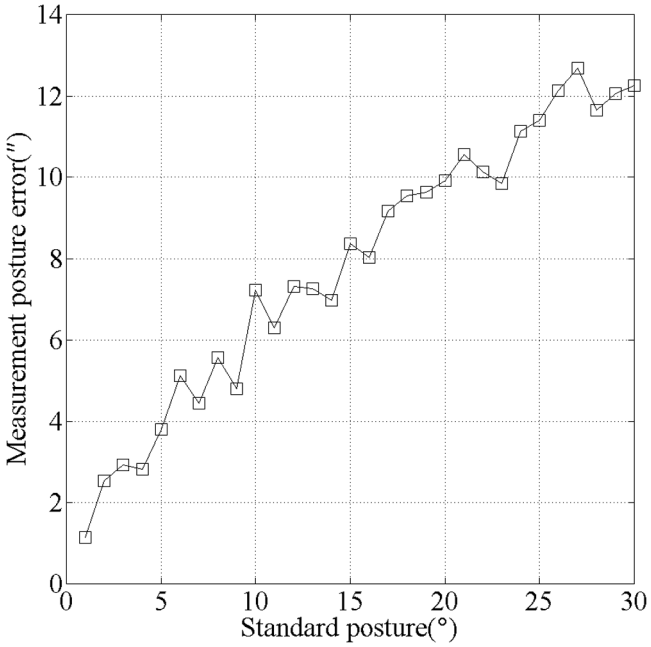

Figure 5. 0°–30° posture measurement errors of the simulation experiment.

Figure 6. Layout of the experiment instrument.

For ease of comparison, we record the changes in the horizontal rotation angle of the turntable in the actual experiment. It is necessary to project plane $A_iB_iC_i$ to the first plane $A_1B_1C_1$ of the turntable during the posture calculation. The normal vector of the first plane $A_1B_1C_1$ is denoted as $\vec{n}\,(x_n, y_n, z_n)$, and A_i, B_i, C_i after projection are indicated as $A_i'(x_{A_i'}, y_{A_i'}, z_{A_i'})$, $B_i'(x_{B_i'}, y_{B_i'}, z_{B_i'})$, $C_i'(x_{C_i'}, y_{C_i'}, z_{C_i'})$.

A_i', B_i', C_i' coordinates are calculated and fitted to the circle, and the center coordinates of circle O_A, O_B, O_C are obtained. The rotation angles θ_{A_i}, θ_{B_i}, θ_{C_i} are computed by calculating the angles between the canters of each ring and the corresponding projection point vectors. Then, the posture of measuring plane θ_i is the mean value of θ_{A_i}, θ_{B_i}, θ_{C_i}

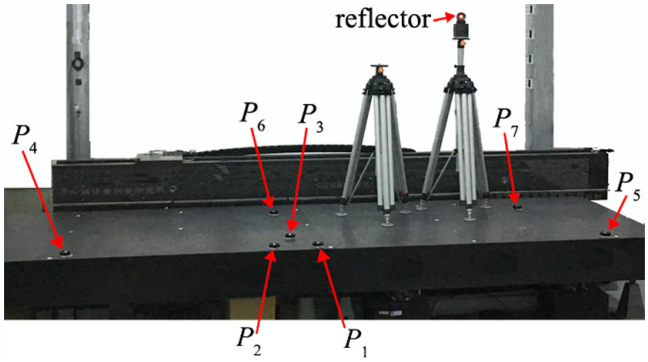

Figure 7. Layout of the reference lengths.

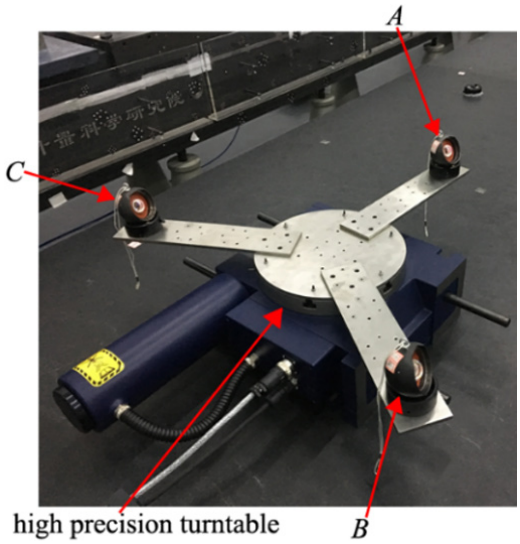

Figure 8. Posture accuracy verification experiments.

$$\theta_{k_i} = \arccos\left(\frac{\overrightarrow{O_k k_i'} \cdot \overrightarrow{O_k k_1'}}{|\overrightarrow{O_k k_i'}||\overrightarrow{O_k k_1'}|}\right), k = A, B, C. \quad (2.27)$$

4. Simulation

To verify the feasibility and accuracy of the posture measurement method, we conduct simulation experiments. As shown in figure 2, we establish the coordinate system and give the measurement center coordinates of six laser tracers.

As shown in figure 4, we create three layers of scatter points in a rectangular area of 3 m × 3 m × 3 m. There are nine points in each layer, showing a uniform chessboard distribution, with a total of 27 points in the three layers, and then we add the initial fixed points A_0, B_0, C_0, with a total of 30 points. We calculate the initial lengths between the initial points A_0, B_0, C_0 and the six laser tracers $S_j, j = 1, \ldots, 6$, and calculate the variations of the lengths Δl_{jA_i}, Δl_{jB_i}, Δl_{jC_i} between each point to six laser tracer lengths from the initial lengths. These data are theoretical stepwise calibration data. The 18 system parameters l_{10}, l_{20}, l_{30}, l_{40}, l_{50}, l_{60}, x_{S_2}, x_{S_3}, y_{S_3}, x_{S_4}, y_{S_4}, z_{S_4},

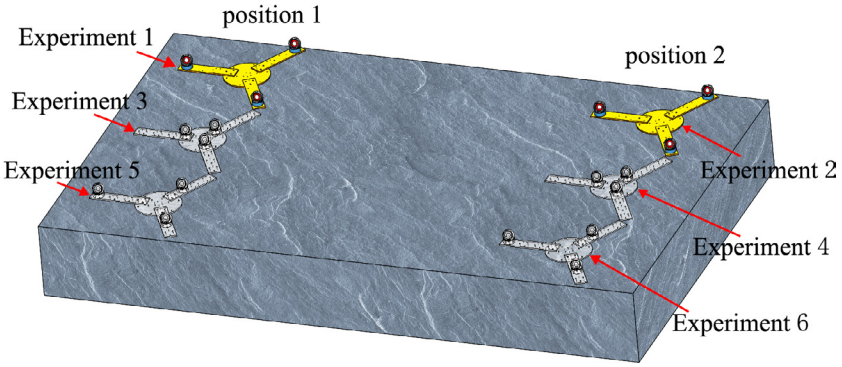

Figure 9. Six experiments on position 1 and position 2.

x_{S_5}, y_{S_5}, z_{S_5}, x_{S_6}, y_{S_6}, z_{S_6} are calculated by analytical stepwise calibration data.

A high precision turntable is used to verify the posture accuracy in the actual experiments. Because the reflector in front will block the laser path of the reflector behind after the turntable is rotated by a certain angle, so the simulation experiment also verifies the posture accuracy of the angle within 30°. Let LT_1, LT_2 and LT_3 track A, LT_4 and LT_5 track B, and LT_6 track C. The lengths between each optical centre of the three reflectors are all 700 mm. First, we generate an initial measuring plane, and then we rotate the initial plane around the centre of the turntable to create a standard posture. Theoretical measuring planes are generated every 1° interval from 1° to 30°, and there are 31 theoretical measuring planes. Based on the 31 theoretical measuring planes, there are variations of the length Δl_{1i}, Δl_{2i}, Δl_{3i}, Δl_{4i}, Δl_{5i}, Δl_{6i} between the theoretical plane i and the six laser tracers from the initial measurements. These data are theoretical planes data.

However, there is inevitably a certain length measurement error in the actual measurement; the theoretical data of the stepwise calibration points and posture planes add noise data. The uncertainty of the laser tracer is $U = 0.2\ \mu m + 0.3\ \mu m\ m^{-1}$. In the simulations, the theoretical data of Δl_{1i}, Δl_{2i}, Δl_{3i}, Δl_{4i}, Δl_{5i}, Δl_{6i} add the random noise within $[0, +U]$, and the lengths of l_{AB}, l_{AC}, l_{BC} add the random noise within $[-100\ \mu m, 100\ \mu m]$. In this simulation, the noise data of l_{AB}, l_{AC}, l_{BC} are $-83\ \mu m$, $25\ \mu m$, and $32\ \mu m$. The length unit of the simulation is in mm, taking the 6th place after the decimal point, so the maximum truncation error is 0.5 nm. These data can be used to calculate the posture of the theoretical measuring planes through the formula in section 3.

As shown in figure 5, in the simulation range of [0°, 30°], the errors are distributed in the field of [1.1″, 12.7″]. The simulation results show that the proposed posture measurement method has a high accuracy in the large-scale measurement range.

5. Experiments of the six-laser multilateral measurement system

To further verify the accuracy of the six-laser multilateral posture measurement system, a stepwise calibration experiment and posture accuracy verification experiment of the system are carried out.

Table 1. Six groups of different experiments.

Experiment	Position	Shape of three reflectors
Experiment 1	Position 1	700 mm regular triangle
Experiment 2	Position 2	700 mm regular triangle
Experiment 3	Position 1	200 mm regular triangle
Experiment 4	Position 2	200 mm regular triangle
Experiment 5	Position 1	Irregular triangle
Experiment 6	Position 2	Irregular triangle

5.1. System parameter self-calibration experiments

Through the coordinates of six laser tracers and the distance between each laser tracer and its corresponding reflectors, the posture of the measuring plane can be calculated. However, it is difficult to accurately calibrate the mutual positional relationship between the six laser tracers by the external measurement method before the actual measurement, which needs to be solved by self-calibration experiments of the system.

The layout of the experimental instrument of the system is shown in figure 6: four laser tracers and two laser trackers are arranged in the experimental space. The maximum height difference of the six instruments is 3.1 m, the maximum distance between left and right is 4.4 m, and the maximum distance between the front and rear is 1.7 m.

In the process of system stepwise calibration, the method of adding the reference length is adopted to improve the accuracy of the system stepwise calibration [18]. As shown in figure 7, there are seven fixed points $P_1, \ldots, P_7$ fixed on the marble plane. P_1 is the initial point A_0 of reflector A, P_2 is the initial point B_0 of reflector B, P_3 is the initial point C_0 of reflector C. The seven fixed points form five reference lengths in two directions, and there are three reference lengths $L_{P_1P_2}$ (from point P_1 to P_2), $L_{P_1P_4}$ (from point P_1 to P_4), and $L_{P_4P_5}$ (from point P_4 to P_5) in one direction. The other two reference lengths are $L_{P_1P_6}$ (from point P_1 to P_6), and $L_{P_5P_7}$ (from point P_5 to P_7) in a different direction.

In the experiments, we select a reflector with a diameter of 75 mm. The length between the experiment location to the origin of the posture measurement system is in the range of [5.3 m, 7.2 m]. Two tripods at different heights are placed

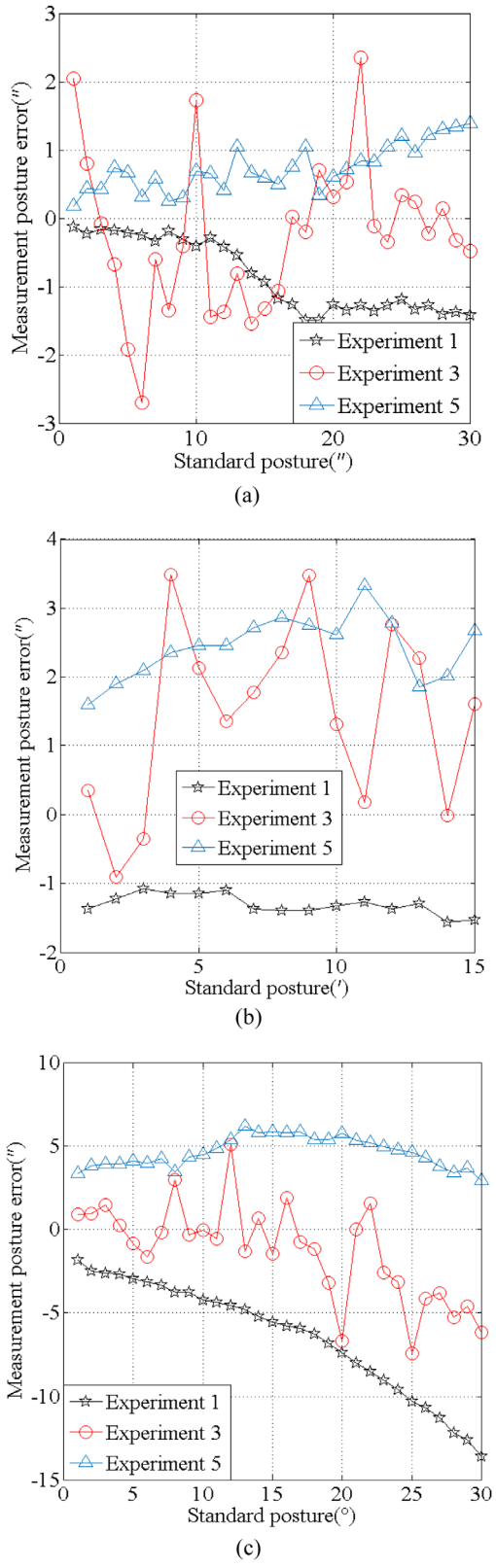

Figure 10. The posture error of three experiments (experiment 1, experiment 3 and experiment 5) at position 1. (a) Range [0″, 30″]; (b) range [0′, 15′]; (c) range [0°, 30°].

on the marble plane to form, along with the marble plane, three measuring planes at different heights. There are seven fixed measurement points on the marble surface, which are respectively $P_1, \ldots, P_7$. In addition, 18 movable measuring points are also evenly distributed in the marble plane. On the plane where the two tripods are located, three measuring points are distributed on each floor. There are 31 measuring points in total distributed on the three measuring planes. First, six instruments are used to track reflector A at the same time, and P_1 is the initial point. Then, moving the reflector, we measure reflector A at 31 measuring points. Secondly, six instruments track reflector B simultaneously. P_2 is the initial point, and we measure reflector B at 31 measuring points. Finally, six instruments track reflector C at the same time. P_3 is the initial point, and we measure reflector C at 31 measuring points. According to the formula in section 3, the system parameters are solved by the measurement data.

5.2. Posture accuracy verification experiments

The posture accuracy verification experiments use a high precision turntable, as shown in figure 8. We place a high-precision turntable on the marble plane with a resolution of 0.1″. Three fixed points are placed on the turntable to position the reflectors A, B, C. The distance between three fixed points l_{AB}, l_{AC} and l_{BC} are calibrated in advance.

The reflectors A, B, C are placed at the fixed points P_1, P_2, P_3 respectively in the experiments. LT_1, LT_2 and LT_3 track A, LT_4 and LT_5 track B, and LT_6 tracks C. We move the reflectors A, B, C from P_1, P_2, P_3 to the fixed points of the turntable, and form the first measuring plane, and turn the turntable to create multiple measuring planes. Taking the high-precision turntable as the standard posture, the six-laser multilateral posture measuring system is compared with the standard posture. By adjusting the mutual positional relationship among the three reflectors A, B, C, we let A, B, C form triangles of different shapes, and then the experiments are carried out.

5.3. Experimental data analysis and processing

As shown in figure 9, two positions (position 1 and position 2) are placed on a marble plane of 5 m × 2.5 m—the distance between the two positions is about 4 m. The lengths between the two locations and the origin of the posture measurement system are in the range of [5 m, 7 m].

As shown in table 1, there are six groups of different experiments, and the posture is measured from 1″ to 30″, 1′ to 15′ and 1° to 30° of each test.

Experiment 1, experiment 3 and experiment 5 are performed at position 1. The results of the posture calculation are shown in figure 10.

As shown in figure 10(a), within the measurement range of [0″, 30″], the posture errors of the three groups are distributed in the [−2.7″, 2.4″] range—the average error is −0.1″ and the standard deviation is 1.0″. As shown in figure 10(b), within the measurement range of [0′, 15′], the posture errors of the three groups are distributed in the [−1.6″, 3.5″] range—the average error is −0.9″ and the standard deviation is 1.8″. As shown in figure 10(c), within the measurement range of

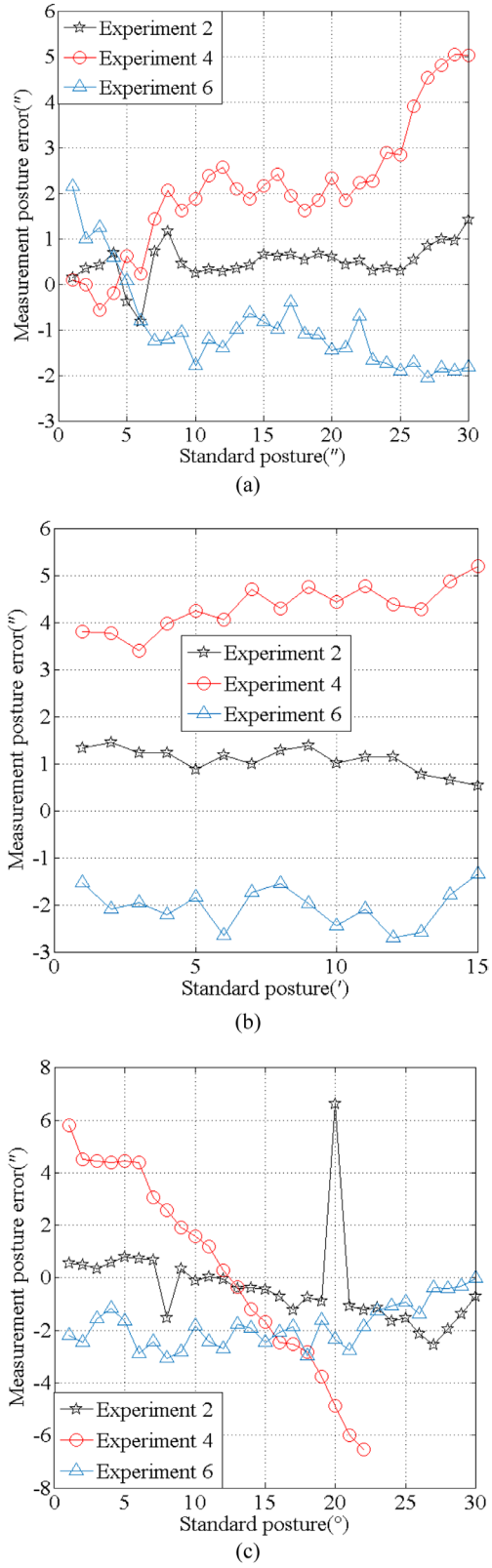

Figure 11. The posture error of three experiments (experiment 2, experiment 4 and experiment 6) at position 2. (a) Range [0″, 30″]; (b) range [0′, 15′]; (c) range [0°, 30°].

[0°, 30°], the posture errors of the three groups are distributed in the [−13.6″, 6.2″] range—the average error is −1.0″ and the standard deviation is 5.2″.

Similarly, experiment 2, experiment 4 and experiment 6 are performed at position 2. The results of the posture calculation are shown in figure 11. Experiment 4 is affected by occlusion of the laser path, and the measurement range is [0°, 22°].

As shown in figure 11(a), within the measurement range of [0″, 30″], the posture errors of the three groups are distributed in the [−2.1″, 5.1″] range—the average error is 0.6″, and the standard deviation is 1.6″. As shown in figure 11(b), within the measurement range of [0′, 15′], the posture errors of the three groups are distributed in the [−2.7″, 5.2″] range—the average error is 1.1″, and the standard deviation is 2.6″. As shown in figure 11(c), within the measurement range of [0°, 30°], the posture errors of the three groups are distributed in the [−6.5″, 6.6″] range—the average error is −0.7″ and the standard deviation is 2.4″.

It is obvious that the posture measurement system has high accuracy in different measurement positions.

6. Conclusions

Given the urgent need for high-accuracy posture measurement in large assembly manufacturing and other fields, a new method of posture measurement based on a six-laser multilateral measurement system is proposed in this paper. After the completion of the system, the system parameters need to be calibrated, but there is no redundant information in the six-laser tracer multilateral posture measuring system, and the traditional self-calibration method cannot be used. Therefore, a stepwise calibration method is proposed to achieve the system calibration. In the actual experiment, the accuracy of the posture measurement system is verified by using a high-precision turntable. A total of six tests were carried out at two different locations in a range of [5 m, 7 m]. The experimental results show that the posture error is distributed in [−13.6″, 6.2″] in a measurement range of [0°, 30°] at position 1, and the posture error is distributed in [−6.5″, 6.6″] in a measurement range of [0°, 30°] at position 2. The experiments prove that the new posture measurement method can realize high-accuracy posture measurement on a large scale.

In future research, we will focus on the algorithm of posture and the distribution of spatial uncertainty. We will also study the influence of different measurement ranges and different positions of reflectors on the accuracy of posture measurement, and find the optimal reflector positions and the best measurement position. Further, due to the limitations of the current verification method, the accuracy of the measurement range in [0°, 30°] can be verified. In subsequent work, the verification method can be improved to verify the accuracy of other measurement ranges.

Acknowledgments

The work is supported by the National Key Research and Development Project of China (Grant No. 2017YFF0204802), and the Fundamental Research Funds of National Institute of Metrology, China (Grant No. AKY1701).

ORCID iDs

Jihui Zheng https://orcid.org/0000-0002-5068-0505
Dongjing Miao https://orcid.org/0000-0002-6849-2238

References

[1] Li M and Yu J P 2017 Status and development of geometric measurement in Industry *Chin. J. Sci. Instrum.* **38** 2959–71
[2] Muelaner J E, Wang Z, Keogh P S, Brownell J and Fisher D 2016 Uncertainty of measurement for large product verification: evaluation of large aero gas turbine engine datums *Meas. Sci. Technol.* **27** 115003
[3] Chen Y and Yue S 2011 Pose measurement base on machine vision for the aircraft model in wire-driven parallel suspension system *Energy Procedia* **13** 6586–92
[4] Wang C, Huang F, Wang X and Chen L 2014 Single camera stereo vision coordinate measurement in parts pose recognization on CMM *Optical Design & Testing VI* **2014** 92720P
[5] Gao Y B, Liu S F, Atia M and Noureldin A 2015 INS/GPS/LiDAR integrated navigation system for urban and indoor environments using hybrid scan matching algorithm *Sensors* **15** 23286–302
[6] Gao Y, Lin J R, Yang L H and Zhu J G 2016 Development and calibration of an accurate 6-degree-of-freedom measurement system with total station *Meas. Sci. Technol.* **27** 125103
[7] Nubiola A and Bonev I A 2013 Absolute calibration of an ABB IRB 1600 robot using a laser tracker *Robot. Comput.-Integr. Manuf.* **29** 236–45
[8] Muralikrishnan B, Phillips S D and Sawyer D S 2016 Laser trackers for large scale dimensional metrology: a review *Precis. Eng.* **44** 13–28
[9] Wan A, Xu J, Miao D and Chen K 2017 An accurate point-based rigid registration method for laser tracker relocation *IEEE Trans. Instrum. Meas.* **66** 254–62
[10] Xiong Z, Zhu J G, Yang X Y and Ye S H 2011 A novel laser multidirection network measurement system *2nd Int. Conf. on Digital Manufacturing & Automation* vol 10 pp 89–92
[11] Shi S D, Yang L H, Lin J R, Ren Y J, Guo S Y and Zhu J G 2018 Omnidirectional angle constraint based dynamic six-degree-of-freedom measurement for spacecraft rendezvous and docking simulation *Meas. Sci. Technol.* **29** 45005
[12] Huo J, Yun H and Yang M 2017 Measurement and error analysis of moving target pose based on laser projection imaging *Acta Photonica Sin.* **46** 912001
[13] Tian L D, Liu C H, Zhao J K, Duan Y X, Pan L, Zhang H X, Duan T, Long J B and Wang Z F 2014 Indoor test method of attitude measurement accuracy of photoelectric theodolite *Acta Opt. Sin.* **34** 0812002
[14] Linares J M, Chaves-Jacob J, Schwenke H, Longstaff A, Fletcher S, Flore J, Uhlmann E and Wintering J 2014 Impact of measurement procedure when error mapping and compensating a small CNC machine using a multilateration laser interferometer *Precis. Eng.* **38** 578–88
[15] Gomez-Acedo E, Olarra A, Zubieta M, Kortaberria G, Ariznabarreta E and Lacalle L 2015 Method for measuring thermal distortion in large machine tools by means of laser multilateration *Int. J. Adv. Manuf. Technol.* **80** 523–34
[16] Ezedine F, Linares J M, Sprauel J M and Chavesjacob J 2016 Smart sequential multilateration measurement strategy for volumetric error compensation of an extra-small machine tool *Precis. Eng.* **43** 178–86
[17] Wendt K, Franke M and Härtig F 2012 Measuring large 3D structures using four portable tracking laser interferometers *Measurement* **45** 2339–45
[18] Miao D J, Wang G L, Li J S, He M Z and Kang Y 2016 An improved self-calibration algorithm for multilateration coordinates measuring system *8th Int. Symp. on Advanced Optical Manufacturing & Testing Technology* p 9684
[19] Miao D J, Li J S, Zheng J H, Li L F, Jiang Y L and Kang Y 2017 Study on self-calibration algorithm and simulation for large-scale posture measurement system based on multilateral method *Acta Metrol. Sin.* **38** 73–8
[20] Zhuang H, Li B and Roth Z S 1992 Self-calibration and mirror center offset elimination of a multi-beam laser tracking system *Robot. Auton. Syst.* **9** 255–69
[21] Daubechies I, Devore R and Fornasier M 2010 Iteratively reweighted least squares minimization for sparse recovery *Commun. Pure Appl. Math.* **63** 1–38